

# The influence of firing profile and additives on the PTCR effect and microstructure of BaTiO<sub>3</sub> ceramics

BI-SHIOU CHIOU

*Institute of Electronics, National Chiao Tung University, Hsinchu, Taiwan*

CHAO-MING KOH, JENQ-GONG DUH

*Department of Materials Science and Engineering, National Tsing Hua University, Hsinchu, Taiwan*

Nonstoichiometric BaTiO<sub>3</sub> PTCR type materials are investigated with various amounts of MnO<sub>2</sub>, Sb<sub>2</sub>O<sub>3</sub> and MgO dopants. Specimens fired with a nonisothermal rate-controlled sintering profile exhibit a rather fine and uniform microstructure as compared to those processed by conventional sintering techniques. The temperature at which the resistivity anomaly begins is observed to decrease with Sb<sub>2</sub>O<sub>3</sub> and MgO contents. The Curie point of BaTiO<sub>3</sub>-based ceramics can be altered by addition of Sb<sub>2</sub>O<sub>3</sub>, and the dielectric peak is maintained by the presence of MgO additive. Magnesium ions act as acceptors in the BaTiO<sub>3</sub> lattice, while antimony ions as donors. The presence of magnesium compensates some of the antimony, hence the doped-BaTiO<sub>3</sub> semiconductive region is pushed to higher contents.

## 1. Introduction

Doped, *n*-type barium titanate ceramics exhibit an abrupt rise in resistivity near the Curie point: the so-called positive temperature coefficient resistivity (PTCR) effect. This resistivity anomaly renders barium titanate useful in various applications [1]. Many studies have been undertaken to investigate the variables which affect the production of the PTCR phenomena [1–16]. The PTCR effect of BaTiO<sub>3</sub> ceramics is extremely sensitive to the concentration and the distribution of the trace additives, to the impurities in the raw materials, and also to the firing condition.

Intrinsically, barium titanate is an insulator but it becomes a semiconductor with the addition of impurities which make chemical defects in the BaTiO<sub>3</sub> lattice provide free electrons for conduction. The U-shaped relation of the dopant ion content and the resistivity of semiconductive BaTiO<sub>3</sub> is well known [4]. Generally, the minimum resistivity exists at 0.3 mol % content of antimony dopant [2]. The microstructure of barium titanate ceramics strongly depends on the history of the firing process. For line voltage applications, a microstructure with fine and uniform grain size is preferred. The purpose of this study is to investigate the PTCR effect of BaTiO<sub>3</sub> ceramics with various amounts of MnO<sub>2</sub>, MgO and Sb<sub>2</sub>O<sub>3</sub> dopants. Different sintering profiles are employed. The relations between the electrical properties and the microstructures of barium titanate will be investigated.

## 2. Experimental procedures

Fig. 1 represents a flow chart of the material fabrication process. The BaTiO<sub>3</sub> powder was prepared by

solid state reaction of BaCO<sub>3</sub> and TiO<sub>2</sub> (reagent grade, Merck & Co., Inc., Darmstadt, Federal Republic of Germany) in the molar ratio of 1:1.01. Excess TiO<sub>2</sub> was added to obtain a TiO<sub>2</sub>-rich liquid phase during sintering [17]. The BaCO<sub>3</sub>, TiO<sub>2</sub> powders together with ethyl alcohol were mixed for 24 h in an alumina ball mill. After drying, the mixture was calcined within an alumina crucible at 1100°C for 1 h, then crushed into powders and sieved through a 200 mesh screen. Appropriate amounts of MnO<sub>2</sub>, Sb<sub>2</sub>O<sub>3</sub> and MgO (Merck, reagent grade) were introduced and mixed with the titanate excess BaTiO<sub>3</sub> powders by the same procedure mentioned above. Powder was then pressed into a disc-shaped specimen, 10 mm in diameter and 2 mm in thickness. Sintering was carried out with two types of firing profiles. The sintering temperatures were chosen to be 1250, 1300, 1400 and 1450°C, while the sintering times were 15, 30 and 60 min. The cooling rate was 150°C h<sup>-1</sup>. After sintering, electrodes were applied to the specimens by rubbing indium–gallium alloy on both surfaces.

The resistance of samples was measured by a UF-1030 digital multimeter (Yue-Hong Electronics Co., Taipei, Taiwan, applied voltage less than 9 V) and the capacitance of samples was measured with the HP4274A LCR meter (Hewlett Packard) at 1 KHZ and 0.5 V.

## 3. Results and discussion

### 3.1. Sintering conditions

#### 3.1.1. Sintering temperature

The effect of sintering temperature on the microstructure of the sample is shown in Fig. 2. For samples sintered at 1250°C for 1 h, no significant grain growth

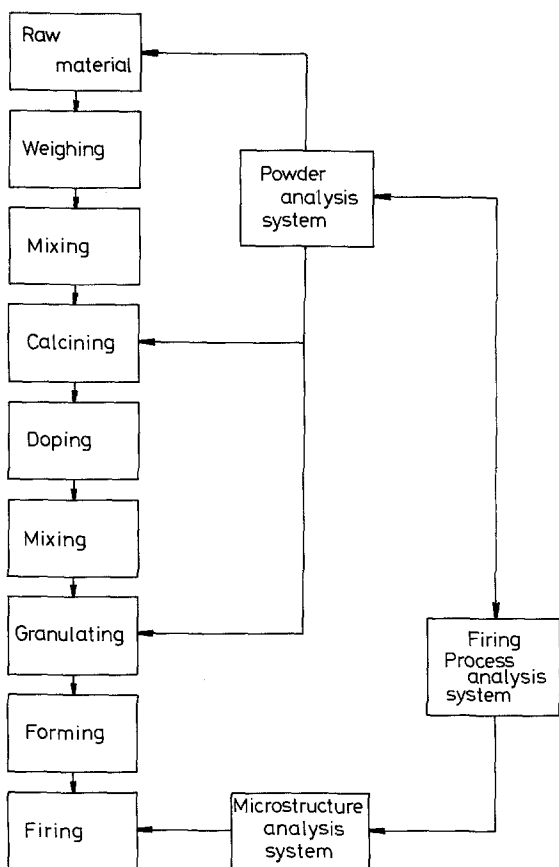


Figure 1 Flow chart of material fabrication process.

was observed. Apparent grain growth started at a temperature higher than 1250°C, and abnormal grain growth was detected at 1300°C and higher temperatures. Samples sintered at 1400 and 1450°C appear to have a smaller grain size than those sintered at 1350°C. This implies that the densification mechanism prevails at high temperature sintering of BaTiO<sub>3</sub> ceramic [18, 19]. Based on the phase diagram of

TiO<sub>2</sub>-BaTiO<sub>3</sub> [20], it is indicated that there exists a eutectic point around 1320°C and liquid phase generally appears at temperatures above 1320°C. The densification at high temperature for TiO<sub>2</sub>-rich BaTiO<sub>3</sub> specimens employed in this study is considered to be the result of liquid phase sintering when the sintering temperature is higher than the eutectic temperature.

Fig. 3 shows the resistivity as a function of the sintering temperature for BaTiO<sub>3</sub> ceramics with 0.05 mol % MnO<sub>2</sub>, 1 mol % Sb<sub>2</sub>O<sub>3</sub> and 1 mol % MgO dopants. It is observed that the room temperature resistivity increases with the sintering temperature. The magnitude of PTCR is of the same order for samples sintered at 1300, 1400 and 1450°C. It appears that sintering temperature only affects the microstructure and the room temperature resistivity of the BaTiO<sub>3</sub> ceramics.

### 3.1.2. Heating rate

Two types of firing profiles as shown in Fig. 4 are employed in this study. The conventional isothermal profile has a constant heating rate of 60°C min<sup>-1</sup> from room temperature up to the sintering temperature of 1400°C, while the controlled one has an initial heating rate of 120°C min<sup>-1</sup> to 1200°C, with 5 min stay at 1200°C and then to the sintering temperature at 120°C min<sup>-1</sup>.

The controlled firing resulted in finer grain size and more uniform grains than the conventional one. Abnormal grain growth is observed for the conventional isothermal heating as shown in Fig. 5. The results are similar to that obtained by Mostaghaci and Brook [18, 19]. If the enthalpy associated with the densification process ( $\Delta H_d$ ) is larger than that associated with the grain growth process ( $\Delta H_g$ ), then a short high temperature firing is preferred to assure a fine

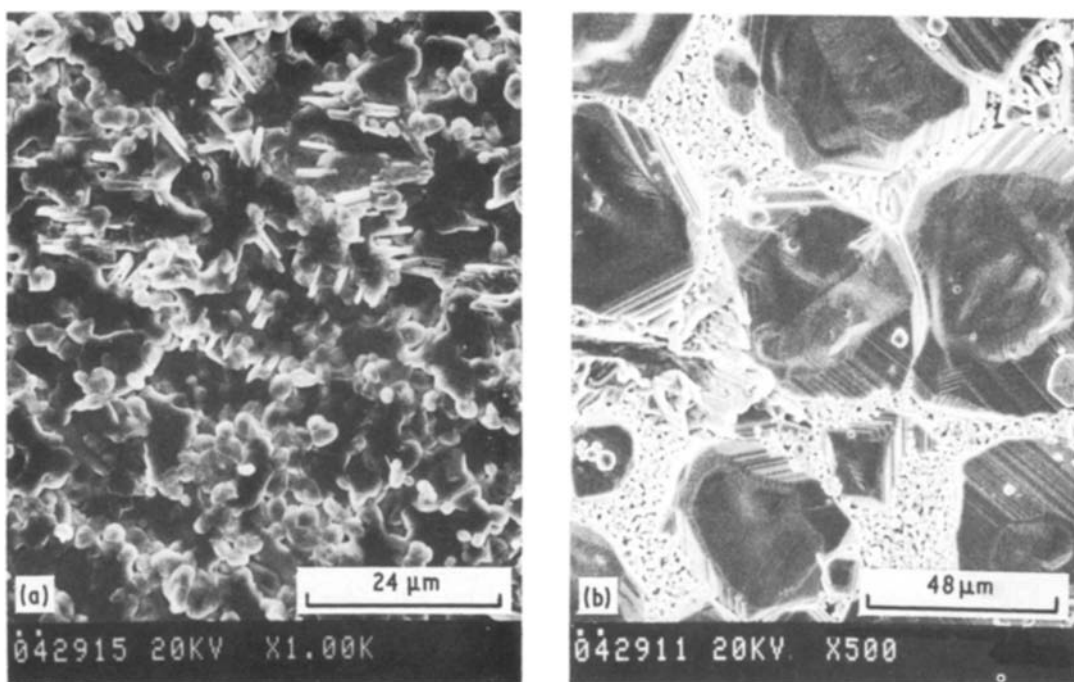


Figure 2 The microstructures of BaTiO<sub>3</sub> with 1 mol % Sb<sub>2</sub>O<sub>3</sub> and 1 mol % MgO sintered at different temperatures and times. (a) 1250°C, 1 h; (b) 1350°C, 30 min; (c) 1300°C, 30 min; (d) 1400°C, 15 min; (e) 1450°C, 15 min.

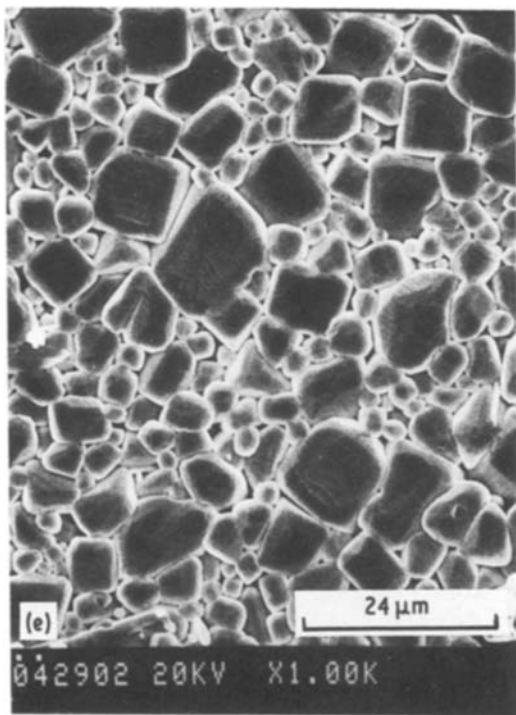
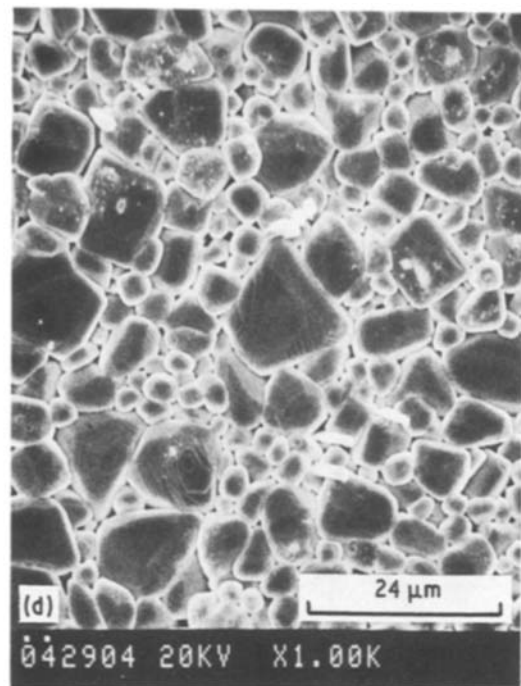
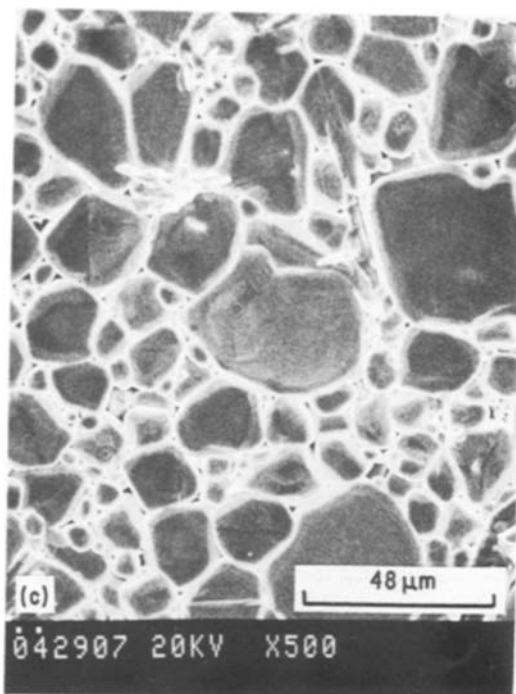


Figure 2 Continued.

grain microstructure. In the controlled firing, the specimen is heated at a low temperature, 1200° C, for a period of 5 min to assure that there is a negligible degree of grain growth. The sample is then heated up rapidly through the low temperature region where the coarsening mechanism is dominant to the region where the densification mechanism takes over. As a result, a fine grain, uniform microstructure is achieved.

There is no appreciable difference in PTCR and the room temperature resistivity between samples sintered with conventional heating and with controlled heating. It appears that the heating rate only affects the microstructure.

### 3.2. Additives

The additives employed in this study are  $\text{MnO}_2$ ,  $\text{MgO}$

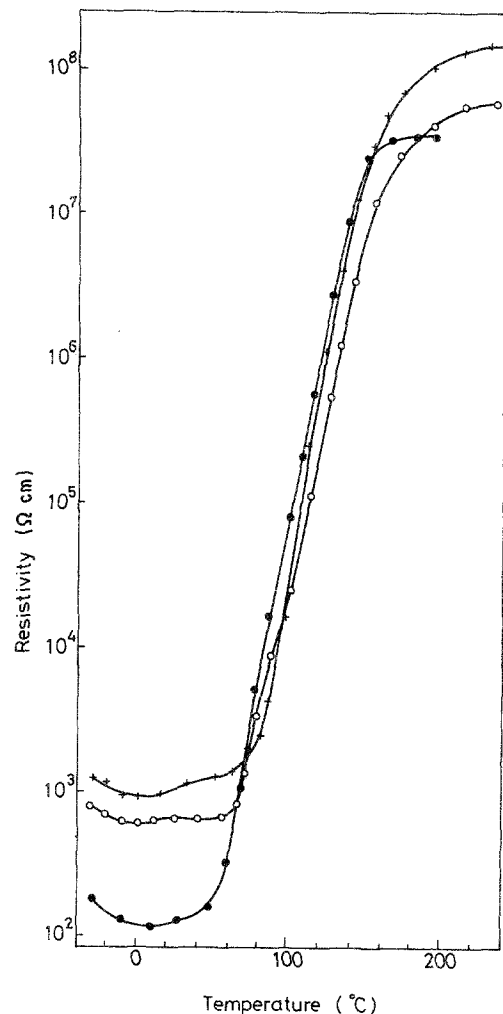


Figure 3 Resistivity as a function of temperature for  $\text{BaTiO}_3$  doped with 0.05 mol %  $\text{MnO}_2$ , 1 mol %  $\text{Sb}_2\text{O}_3$ , and 1 mol %  $\text{MgO}$ . Sintering conditions: +, 1450° C, 15 min; O, 1400° C, 15 min; ●, 1300° C, 60 min.

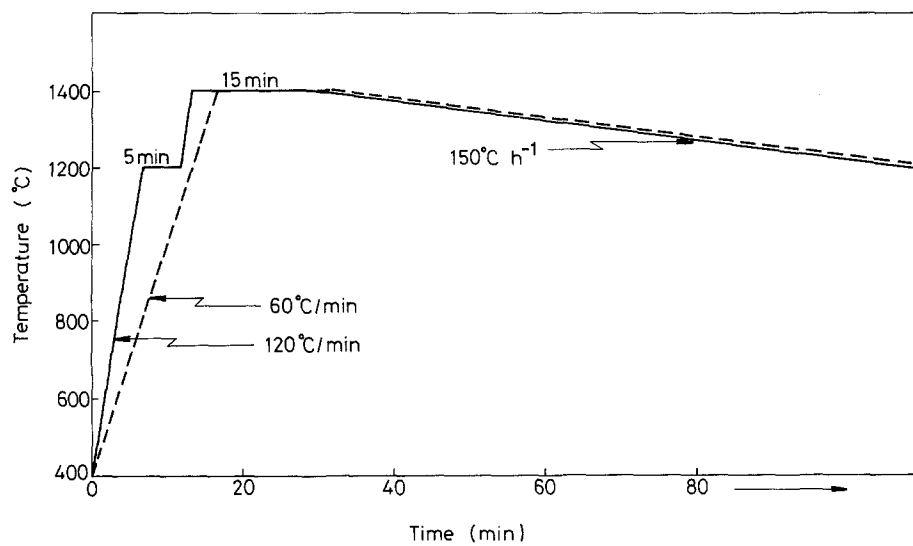


Figure 4 Firing profiles employed in this study. —, controlled; ----, conventional.

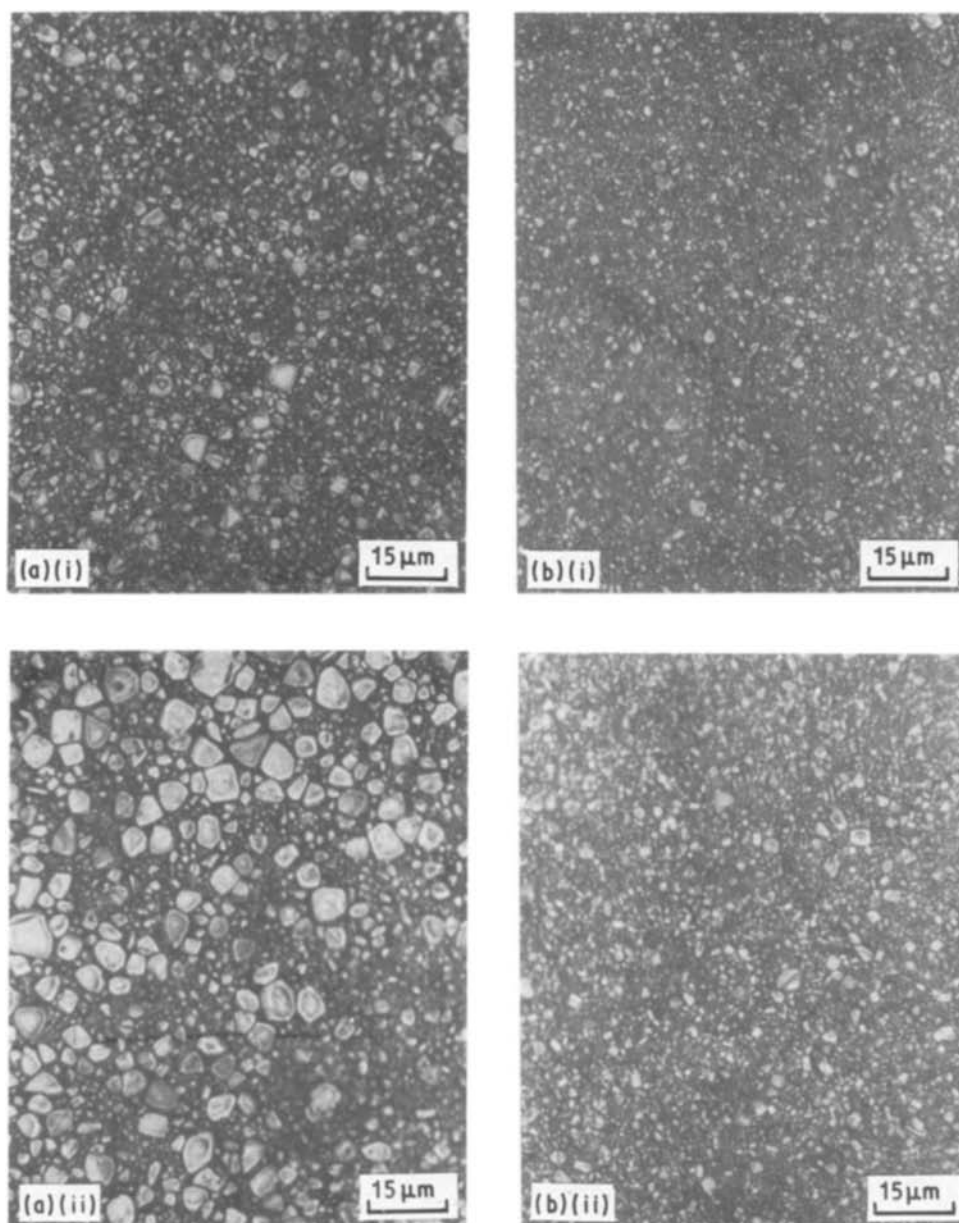


Figure 5 The microstructure of the as-fired sample, composition  $\text{BaTiO}_3$  with  $X$  mol%  $\text{MnO}_2$ , 1 mol%  $\text{Sb}_2\text{O}_3$ , and 1 mol%  $\text{MgO}$ . (a) Conventional firing; (b) controlled firing; (i)  $X = 0$ ; (ii)  $X = 0.05$ .

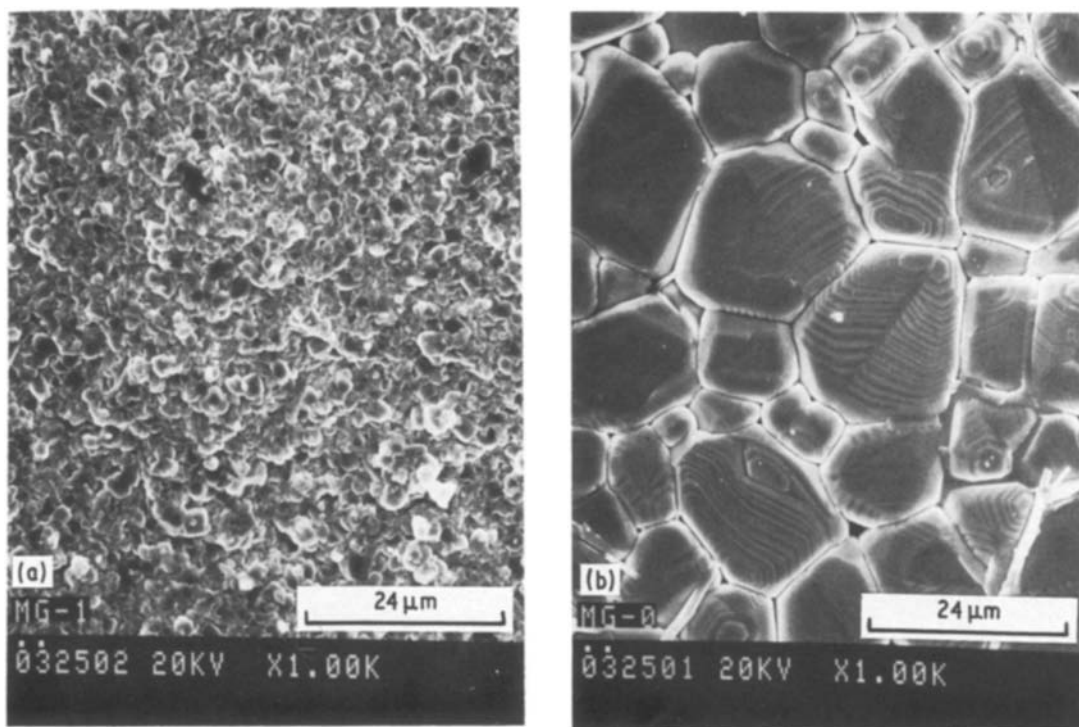


Figure 6 Microstructure of BaTiO<sub>3</sub> with and without MgO (a) with 1 mol % MgO; (b) without MgO. Samples sintered at 1400° C for 15 min.

and Sb<sub>2</sub>O<sub>3</sub>. The content of MnO<sub>2</sub> in most specimens is 0.05 mol %.

MgO is widely used as a grain growth inhibitor for many ceramics. One mole percent of MgO addition retards BaTiO<sub>3</sub> grain growth as shown in Fig. 6. A uniform, fine-grain microstructure is obtained for the MgO-doped sample. Adding Sb<sub>2</sub>O<sub>3</sub> to the MgO-doped BaTiO<sub>3</sub> seems to affect the microstructure of the specimens. Grains larger than 20 μm are observed for the 0.5 mol % Sb<sub>2</sub>O<sub>3</sub>-doped samples. Abnormal grain growth is observed for samples doped with 0.5,

0.88 and 1 mol % Sb<sub>2</sub>O<sub>3</sub>, while the 1.25 and 1.5 mol % Sb<sub>2</sub>O<sub>3</sub>-doped samples have more uniform microstructures, as shown in Fig. 7. As to the electrical properties, only samples with 0.88 and 1 mol % Sb<sub>2</sub>O<sub>3</sub> exhibit a PTCR effect as shown in Fig. 8. A composition of 1 mol % Sb<sub>2</sub>O<sub>3</sub> fired with a controlled heating profile, has a PTCR effect of 10<sup>5.5</sup> and the temperature of initial resistivity rising point is observed to be around 90° C. The other compositions have room temperature resistivities of larger than 10<sup>10</sup> Ωcm. The dielectric constant and resistivity as a

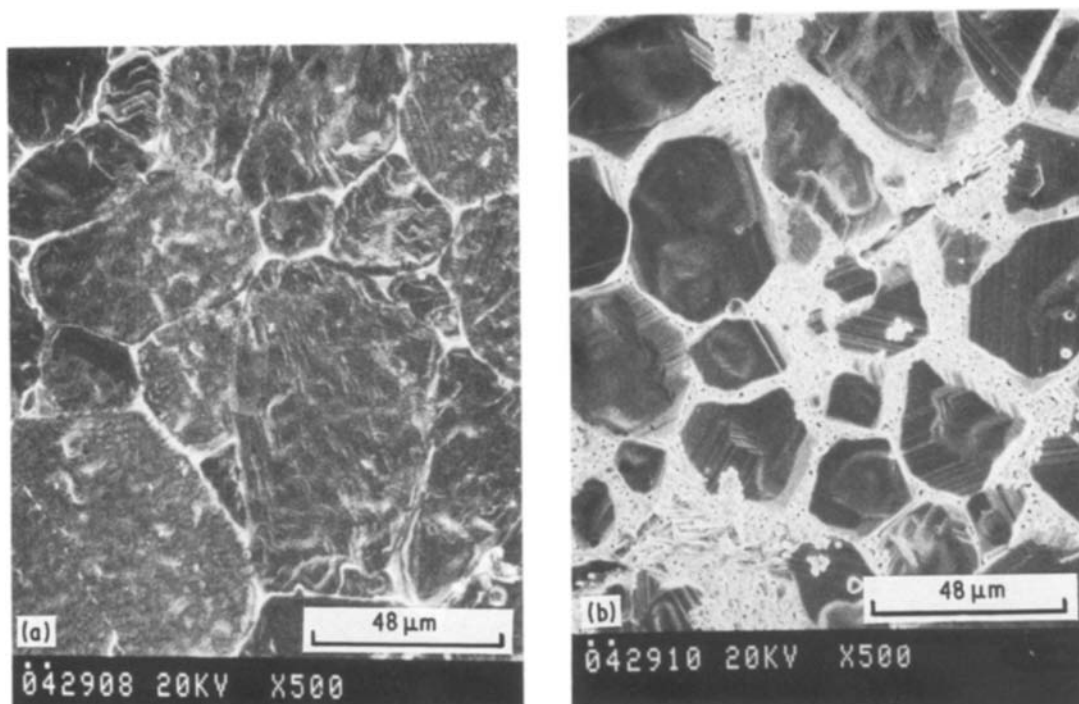


Figure 7 Microstructure of BaTiO<sub>3</sub> doped with 1 mol % MgO and X mol % Sb<sub>2</sub>O<sub>3</sub>. Samples sintered at 1300° C for 60 min. (a) X = 0.5; (b) X = 0.88; (c) X = 1.0; (d) X = 1.25; (e) X = 1.5.

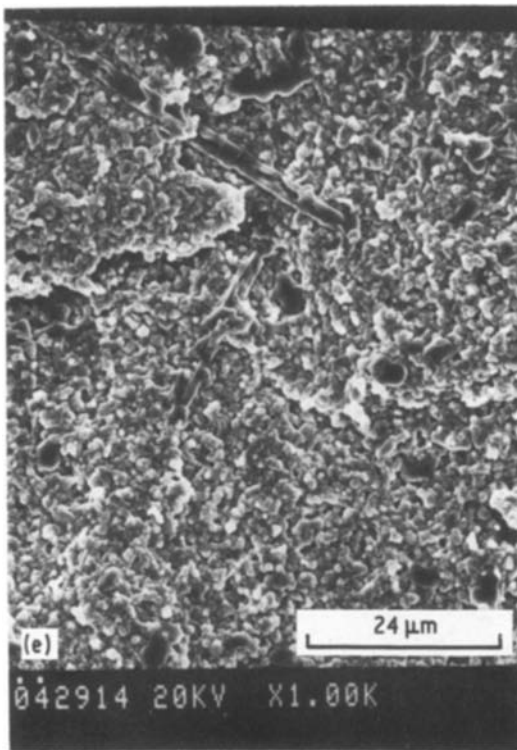
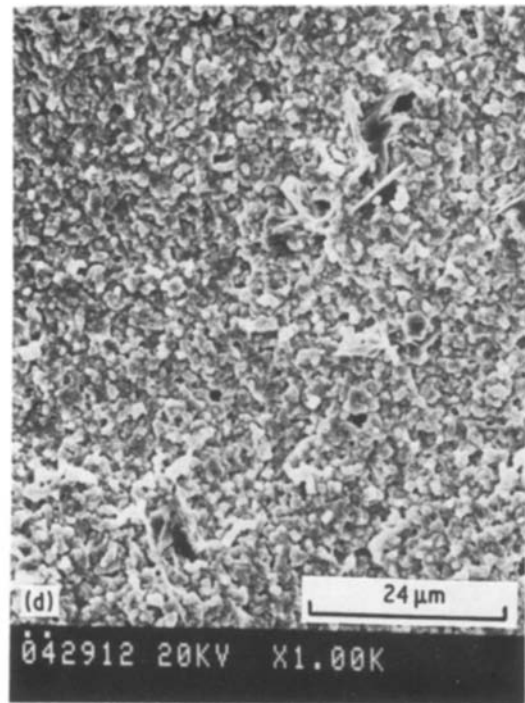
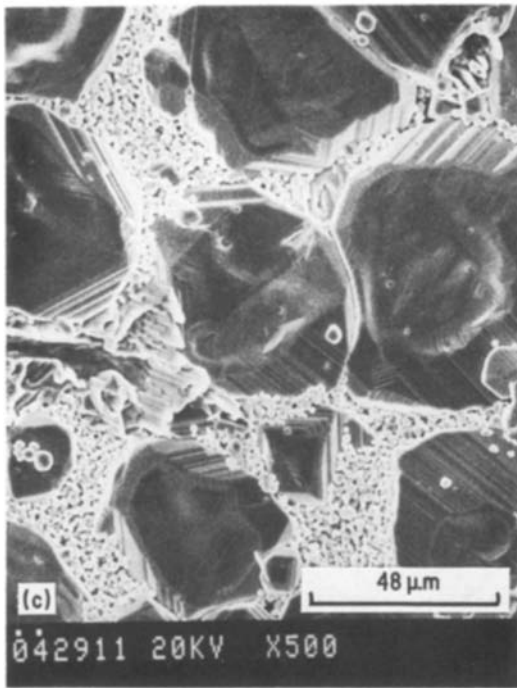


Figure 7 Continued.

function of temperature for the  $\text{Sb}_2\text{O}_3$ -doped samples are given in Fig. 9. The dielectric peaks of the 0.5 and 0.88 mol %  $\text{Sb}_2\text{O}_3$  samples are around  $90^\circ\text{C}$ , and orthorhombic to tetragonal transition temperature for these two compositions are around  $10^\circ\text{C}$ . Samples doped with 1.25 and 1.75 mol %  $\text{Sb}_2\text{O}_3$  exhibit similar behaviour, nevertheless the dielectric peaks are relatively small for these two compositions.

Previous works by Heywang and others suggest that there is an optimal antimony content range for  $\text{BaTiO}_3$  to become semiconductive and that beyond that range, an insulator is obtained instead [2]. The antimony content range in this study is found to be around 2 at %, which is larger than that observed by

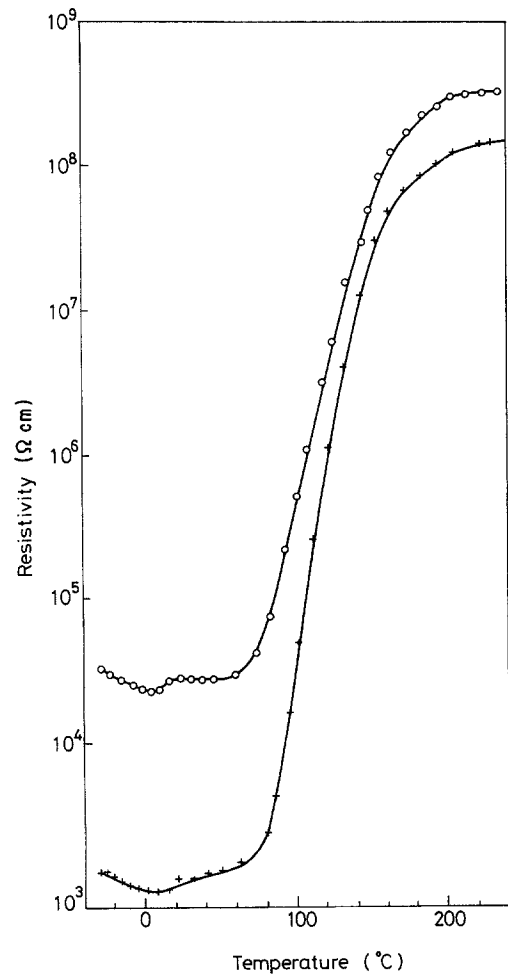


Figure 8 Resistivity as a function of temperature for  $\text{BaTiO}_3$  doped with 0.05 mol %  $\text{MnO}_2$ , 1 mol %  $\text{MgO}$ , and  $X$  mol %  $\text{Sb}_2\text{O}_3$ . Sintering conditions:  $1450^\circ\text{C}$ , 15 min. Controlled heating, +,  $x = 1$ ; ○,  $X = 0.88$ .



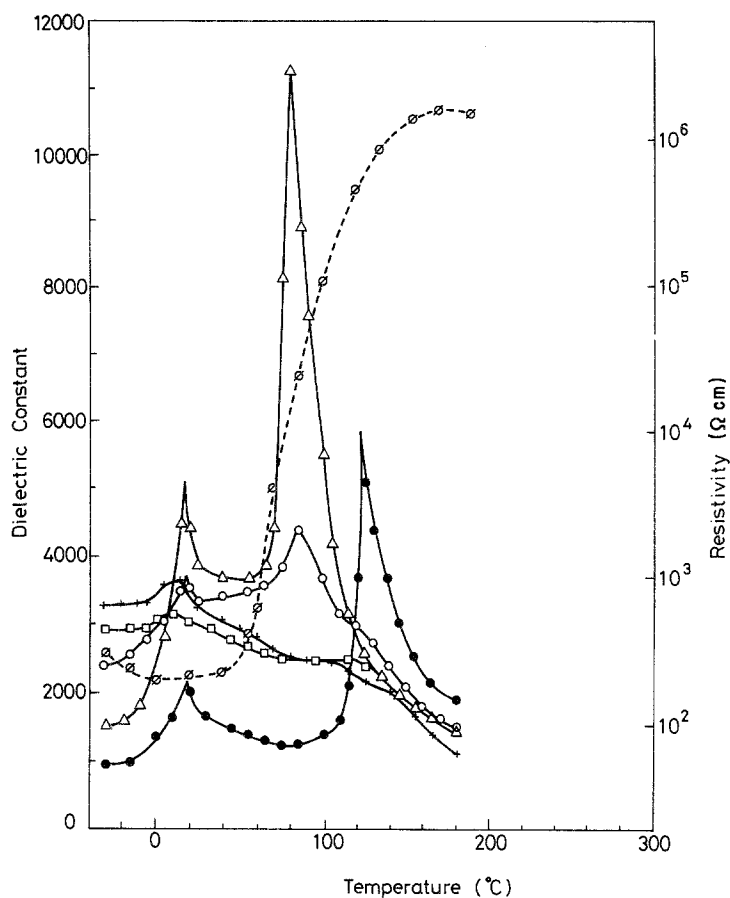


Figure 9 Dielectric constant and resistivity as a function of temperature for BaTiO<sub>3</sub> with 1 mol % MgO and various amounts of Sb<sub>2</sub>O<sub>3</sub>. Sintering conditions: 1300°C, 60 min, controlled heating. Sb<sub>2</sub>O<sub>3</sub> content: ●, 0.0; ○, 0.5; △, 0.75; ∅, 1.0; +, 1.25; □, 1.75. —, Dielectric constant (1 kHz); ----, resistivity.

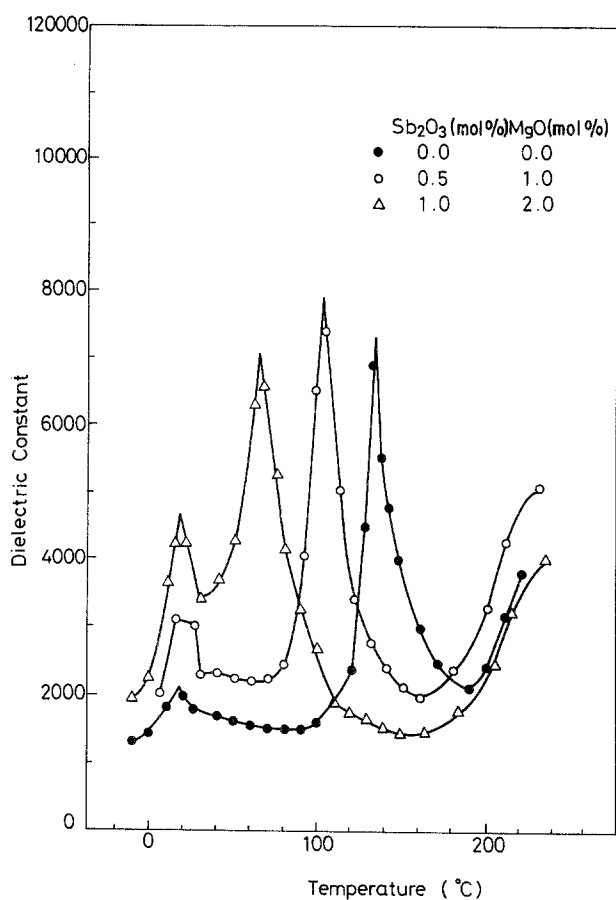


Figure 10 Dielectric constant as a function of temperature for BaTiO<sub>3</sub> doped with equal amounts of antimony and magnesium dopants. Sintering conditions: 1400°C, 15 min, controlled heating.

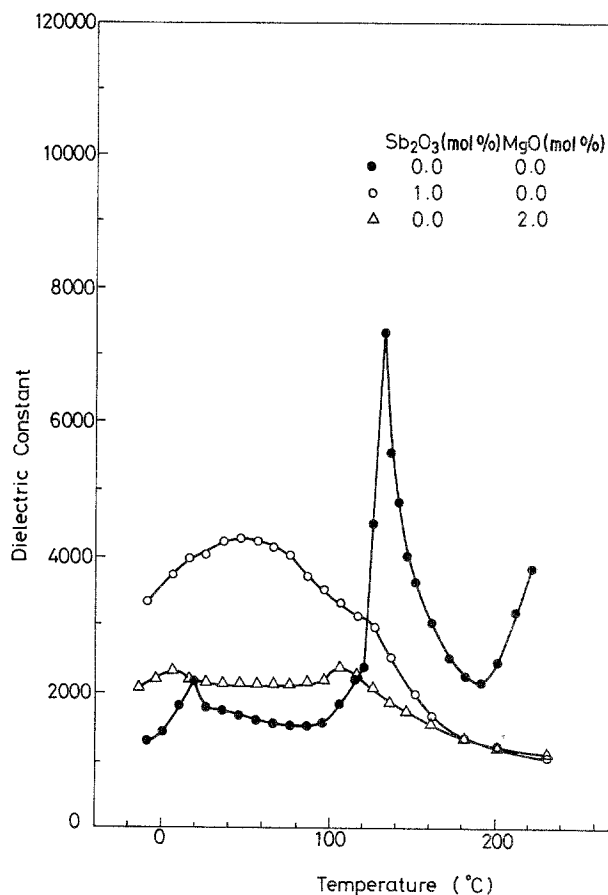


Figure 11 Dielectric constant as a function of temperature for BaTiO<sub>3</sub> doped with various amounts of antimony and magnesium dopants. Sintering conditions: 1400°C, 15 min, controlled heating, 1 kHz.

Heywang [2]. This may be attributed to the presence of 1 mol % MgO. In BaTiO<sub>3</sub> solid solution, the ionic radii of Ba<sup>2+</sup>, Mg<sup>2+</sup>, Sb<sup>5+</sup> and Ti<sup>4+</sup> ions are 0.136, 0.072, 0.061 and 0.061 nm, respectively [21]. As a consequence, Sb<sup>5+</sup> ions tend to occupy the position of Ti<sup>4+</sup> in preference to Ba<sup>2+</sup> ions, while Mg<sup>2+</sup> would replace Ba<sup>2+</sup>. From the resistivities of the 1.75 and 2 mol % Sb-doped samples, as shown in Fig. 8, it is suggested that the ability of magnesium to capture electrons is larger than that of antimony to release electrons. Magnesium ions behave as strong electron acceptors in BaTiO<sub>3</sub> ceramics, hence more antimony is needed to compensate the effect of magnesium. Thus magnesium ions act not only as grain growth inhibitors, but also as electron acceptors in BaTiO<sub>3</sub> ceramics.

There is a combined effect of magnesium and antimony on BaTiO<sub>3</sub> ceramics. From Figs. 9 to 11, it appears that a sharp dielectric peak is obtained only when equal amounts of antimony and magnesium are added. The sample doped with 1 mol % Sb<sub>2</sub>O<sub>3</sub> has a dielectric peak around 65°C, but the ferroelectric–paraelectric (F–P) transition is not as sharp as the undoped BaTiO<sub>3</sub>. For samples doped with 2 mol % MgO, there is an F–P transition around 105°C. The dielectric peak at the F–P transition is smaller than the undoped BaTiO<sub>3</sub> as indicated in Fig. 10. As the solubility of MgO in BaTiO<sub>3</sub> is around 1 mol %, the MgO-rich second phase appears to be one of the reasons for the smaller dielectric peak.

As shown in Fig. 10, the dielectric peak at the F–P transition shifts to  $T = 100^\circ\text{C}$  for samples doped with 0.5 mol % Sb<sub>2</sub>O<sub>3</sub> and 1 mol % MgO, while it shifts to 65°C for samples with 1 mol % Sb<sub>2</sub>O<sub>3</sub> and 2 mol % MgO dopants. Besides, the dielectric peaks for these two compositions are comparable to that of the undoped BaTiO<sub>3</sub>. For samples doped with 1 mol % Sb<sub>2</sub>O<sub>3</sub> and 1 mol % MgO, the resistivity anomaly starts at 60°C as shown in Fig. 9. According to the Heywang model [22], the abrupt rise of resistivity occurs near the FP transition temperature. The results suggest that MgO is not as effective as Sb<sub>2</sub>O<sub>3</sub> in altering the Curie temperature of BaTiO<sub>3</sub> ceramics, and that the antimony presence appears to be the dominant factor for the shift of the dielectric peak.

#### 4. Conclusions

1. BaTiO<sub>3</sub> sintered at 1450°C, for 15 min with a controlled heating profile and 0.05 mol % MnO<sub>2</sub>, 1 mol % MgO, and 1 mol % Sb<sub>2</sub>O<sub>3</sub> additives has a PTCR effect of 10<sup>5.5</sup> and a temperature of initial resistivity rising point at 90°C.

2. The densification sintering mechanism predominates over the grain growth mechanism during the sintering process of BaTiO<sub>3</sub>, above 1400°C with 0.05 mol % MnO<sub>2</sub>, 1 mol % MgO and 1 mol % Sb<sub>2</sub>O<sub>3</sub> dopants.

3. The faster heating rate in the sintering of BaTiO<sub>3</sub> ceramics from 1200 to 1400°C results in a finer and more uniform microstructure than the slower one.

4. The maximum dielectric constant of BaTiO<sub>3</sub> F–P transition can be altered by addition of Sb<sub>2</sub>O<sub>3</sub>. The sharpness of the peak is, however, maintained by the presence of MgO additives.

5. The Mg<sup>2+</sup> ion acts as an acceptor in the BaTiO<sub>3</sub> lattice, which can compensate the donor contribution from antimony and subsequently shifts the doped-BaTiO<sub>3</sub> semiconducting region to higher antimony contents.

#### References

1. B. M. KULWICKI, *Adv. Ceram.* **1** (1981) 138.
2. W. HEYWANG, *J. Amer. Ceram. Soc.* **74** (1964) 484.
3. H. A. SAUER and J. R. FISHER, *ibid.* **43** (1960) 297.
4. T. MASTUOKA, Y. MATSUO, H. SASAKI and S. HAYAKAWA, *ibid.* **55** (1973) 108.
5. M. KUWABARA, *ibid.* **64** (1985) 639.
6. M. KURABAWA, S. SUEMURA and M. KAWAHARA, *ibid.* **64** (1985) 1394.
7. G. GOODMAN, *ibid.* **46** (1963) 48.
8. B. G. BRAHMECHA and K. P. SINHA, *Jpn J. Appl. Phys.* **10** (1971) 496.
9. M. KAHN, *Ceram. Bull.* **50** (1971) 676.
10. T. FUKAMI and H. TSUCHIJA, *J. Appl. Phys.* **50** (1979) 735.
11. M. B. HOLMES, V. A. McCROHAN and W. Y. HOWNG, *Adv. Ceram.* **7** (1983) 145.
12. H. UEOKA and M. YODOGAWA, *IEEE Trans. Manuf. Tech., MFT* **3** (1974) 77.
13. F. C. FULSON and T. C. RETT, *J. Electrochem. Soc.* (1979) 165.
14. H. IHRING, *J. Amer. Ceram. Soc.* **64** (1981) 617.
15. P. KAHN, *ibid.* **54** (1971) 452.
16. M. KUWABARA, *Adv. Ceram.* **7** (1983) 128.
17. H. U. ANDERSON, *J. Amer. Ceram. Soc.* **56** (1973) 605.
18. H. MOSTAGHACI and R. J. BROOK, *J. Brit. Ceram. Soc.* **80** (1981) 148.
19. H. MOSTAGHACI and R. J. BROOK, *Trans. J. Brit. Ceram. Soc.* **82** (1983) 167.
20. E. M. LEVIN, C. R. ROBBINS, H. F. McMURDIE and M. K. RESER, (ed.), "Phase Diagram for Ceramists" (The American Ceramic Society, 1964) p. 98.
21. W. D. KINGERY, H. K. BOWEN and D. R. UHLMANN, "Introduction to Ceramics", (1976) p. 58.
22. W. HEYWANG, *Solid State Electron.* **3** (1961) 51.

Received 20 October 1986  
and accepted 31 March 1987